RSC Advances

ROYAL SOCIETY OF CHEMISTRY

www.rsc.org/advances

Ionic liquid entrapment by electrospun polymer nanofiber matrix as a high conductivity polymer electrolyte

R. S. Datta[a], S. M. Said[a*], S. R. Shahrir[a], Norbani Abdullah[c], M. F. M. Sabri[b], S. Balamurugan[a], Y.Miyazaki[e], K. Hayashi[e], N.A. Hashim[d] ,Umma Habiba[b] ,Amalina M. Afifi[b]

[a]Department of Electrical Engineering, Faculty of Engineering, University of Malaya, 50603 Kuala Lumpur, Malaysia

[b]Department of Mechanical Engineering, Faculty of Engineering, University of Malaya, 50603 Kuala Lumpur, Malaysia

[c]Department of Chemistry, Faculty of Science, University of Malaya, 50603 Kuala Lumpur, Malaysia

[d]Department of Chemical Engineering, Faculty of Engineering, University of Malaya, 50603 Kuala Lumpur, Malaysia

[e]Department of Applied Physics, Tohoku University, Sendai, Japan.

[*]smsaid@um.edu.my
Office: +60379675399
Fax: +60796735316

Abstract

Through external doping, novel conductive polymer nanofibers were successfully fabricated using ionic liquids. In this work, polymer blend of polyvinyl alcohol (PVA) and chitosan (CS) of 4: 1 weight ratio was fabricated in the form of nanofibers through electrospinning and used as a scaffolded membrane to capture room-temperature ionic liquids (RTILs), such as 1-ethyl-3-methylimidazolium chloride (EMIMCl) and 1-butyl-3-methylimidazolium bromide (BMIMBr). The morphological analysis through scanning electron microscope (SEM) showed that the scaffold structure of the electrospun membrane facilitated sufficient trapping of RTILs. This membrane has demonstrated significantly increased conductivity from 6×10^{-6} S/cm to 0.10 S/cm, interestingly surpassing the value of pure ionic liquids, where the polymer chain breathing model has been suggested as a hypothesis to explain the phenomena. The dominance of ions as charge carriers was explained using ionic transference number measurement. The interaction between polymer nanofiber matrix and an ionic liquid has been explained using Fourier-transform infrared spectroscopy (FTIR), where the ionic liquid was found to be physically dispersed in the polymer nanofiber matrix. These materials have also shown some thermoelectric (TE) activity, by demonstrating Seebeck coefficient of up to 17.92 μV/K. The existence of freely movable ions in this type of membrane shows their applications as energy storage/conversion devices, such as organic thermoelectric (TE), sensor, and dye-sensitised solar cell.

1. Introduction

The electrospinning technique is an efficient and popular technique to fabricate polymer nanofibrous materials with high surface-to-volume ratio, controllable compositions, and high porosities for a wide range of applications [1, 2]. The electrospun polymer nanofibers has smaller pores and higher surface area than regular fibers[3]. This techniques provides small particle size distribution helps to achieving better contact between electrode and the electrolyte and decrease the ion diffusion distance[4-5]. Thus far, electrospun polymer nanofibers have been successfully investigated in tissue engineering[6], filtration[7], nanocatalysis[8], biomedical applications[9], biosensors[10], pharmaceutical applications[11], protective clothing[12], and environmental engineering [13, 14]. However, a very few reports were found targeting their applications in energy storage/conversions and generations. Some attempts were found reporting the increased conductivity of the electrospun polymer nanofibers. For example, Chronakis *et al*. reported the electrical conductivity value of 1.2×10^{-5} S/cm for electrospun polypyrrole-poly (ethylene oxide) nanofibrous membrane [15] and the conductivity value of 7.7×10^{-5} S/cm for electrospun hybrid nanofibers of amphiphilic salts was reported by Zhou *et al.*, which showed a great promise to obtain enhanced conductivity in electrospun polymer nanofibers [16]. The fabrication of the nanofibrous scaffold from a variety of natural and synthetic polymers. Biopolymers, in particular have attracted much attention in sustainable energy productions not only for their abundance in nature, but also due to their outstanding biocompatibility and biodegradability; resulting in their widespread use in electrospinning [17].

Chitosan (CS), the N-deacetylated derivative of chitin, has received attention due to its promising prospects in industrial applications. The molecular structure of CS is illustrated in Fig. 1a. CS is a natural polymer, hence it has been a good replacement for the role of synthetic polymers in many polymer industries [18, 19]. The free amino and hydroxyl groups on the backbone provide the opportunity to tuning the properties of CS via organic reactions. It possesses excellent properties such as high charge carrier density, biodegradable, non-toxic, film and fiber forming, cross-linking, bonding ability with heavy metals, etc. Hence, it has been a leading candidate material in many areas of applications such as energy storage/conversion, biomedical applications, wastewater treatment and industrial applications".

Polyvinyl alcohol (PVA) is a naturally non-toxic and water-soluble synthetic polymer. Its biocompatibility, high fibre-forming ability, chemical and thermal stability, and other desirable properties make it ideal for industrial applications. In particular, PVA facilitates blending with various synthetic and biopolymers due to its highly

hydrophilic nature. Importantly, the bio-inertness of PVA determines its extensive use in implantable medical devices [20, 21]. Fig. 1b presents the molecular structure of PVA.

Ionic liquids (ILs) are organic salts that offer substantial promise in the chemical processing and related industries due to their unique physical and chemical properties. ILs are essentially found in the liquid state at room temperature and exhibit high ionic conductivity and extremely low volatility, which make them ideal for device applications [22-25].

In general, polymer membranes formed by the blending of polymers exhibit improved mechanical and physical properties compared with the membranes fabricated from individual materials [21]. In this work, a novel method was approached, where a blend polymer solution of PVA and CS, was fabricated in the form of nanofibers through electrospinning. The electrospun polymer membrane was found to act as a scaffold for trapping the room-temperature ionic liquids (RTILs) (which are the conducting host molecules), such as 1-ethyl-3-methylimidazolium chloride (EMIMCl) (Fig. 1c) and 1-butyl-3-methylimidazolium bromide (BMIMBr), (Fig. 1d), and thus successfully demonstrated significantly increased conductivity with promising Seebeck coefficients. Furthermore, the charge transport was investigated through ionic transference number measurement, participation of PVA/CS/RTIL functional groups in the system was explained using Fourier-transform infrared (FTIR) spectroscopy, and the morphology was investigated using scanning electron microscope (SEM).

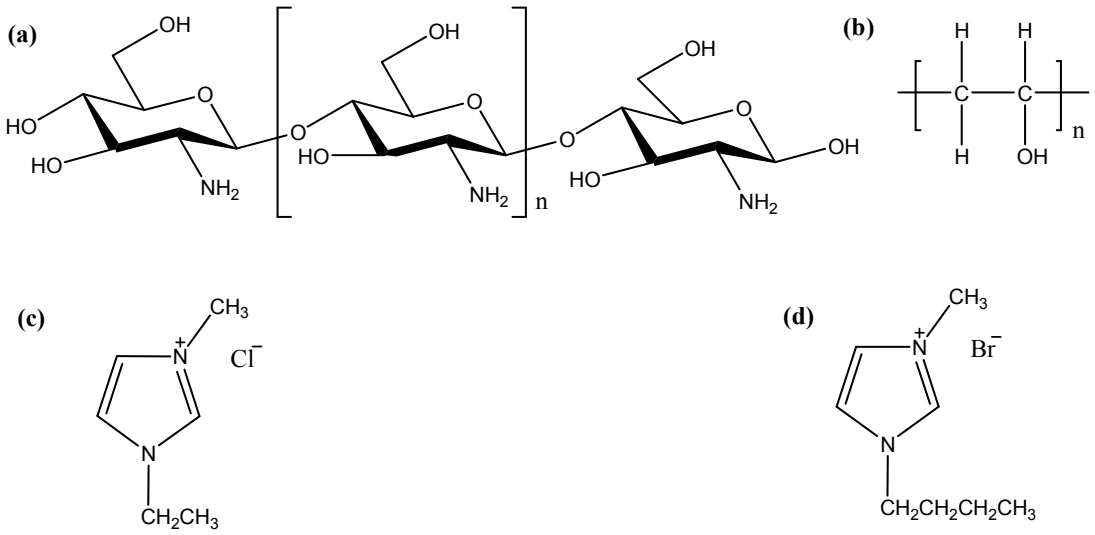

Fig. 1 Molecular structures of (a) CS, (b) PVA, (c) EMIMCl, and (d) BMIMBr.

2. Experimental

2.1. Materials and methods

The polymer CS (SE Chemical Co., Ltd., Japan), Mw=2.4×105 g/mol, degree of deacetylation (DD) =84 %, PVA (Kurray Co. Ltd., Tokyo, Japan), Mw=60000, degree of hydrolysing (DH) =89 %) and ionic liquids (BMIMBr and EMIMCl) (Sigma Aldrich) and acetic acid (Sigma Aldrich) were used as received.

2.1.1. Fabrication of PVA: CS blends

First, 7 wt% CS was dissolved in 90% acetic acid solution in distilled water. On the other hand, 8 wt% PVA was dissolved in distilled water. Finally, PVA: CS weight ratio of 4:1 was prepared as polymer blend solution by stirring for 2 h [26].

2.1.2. Electrospinning parameters

The polymer blend solution was enclosed in a 10 ml plastic syringe. An electrically grounded aluminium (Al) plate wrapped with Al foil was used as the collector. Table 1 lists the parameters used to fabricate PVA: CS nanofibers.

Table 1: Electrospinning parameters used to fabricate PVA:CS nanofibers

wt% (PVA:CS)	Applied Voltage (kV)	Tip-to-Collector Distance (cm)	Feed Rate (ml/h)
4:1	7	10	0.2

2.1.3. Preparation of ionic liquid solutions

Electrolyte solutions were prepared to improve the electrical conduction of the PVA: CS electrospun polymer membranes. Molar concentrations of 1 mol/L and 2 mol/L of imidazolium substituted RTILs were prepared separately using distilled water as the solvent in every set. The solutions were stirred for 1 h at room temperature (25ºC) to ensure proper dissolution.

2.1.4. Preparation of PVA: CS nanofiber-scaffolded ionic liquid membrane

Nanofiber-scaffolded thin polymer membrane of PVA: CS fabricated via electrospinning was immersed in RTIL solutions, individually for 24 h to ensure adequate trapping of RTILs. After immersion, the polymer membranes adhered to glass substrates were stored with silica gel in a Petri dish for 5 days inside a dry cabinet under 40ºC/30% humidity conditions for drying.

2.2. Characterization

2.2.1. Morphological properties

The membrane thicknesses were measured using a KLA TencorP-6 stylus profiler, which is a contact-type measurement technique. The morphological analysis of the nanofiber-scaffolded thin polymer membrane of PVA: CS was conducted using an FEI scanning electron microscope (SEM) in low-vacuum mode.

2.2.2. Electrical properties

The electrical properties of the nanofiber-scaffolded thin polymer membranes of PVA: CS immersed in RTILs were investigated by the four-point probe technique. In four-point probe method, separate pairs of current-carrying and voltage-sensing electrodes eliminate the impedance contribution of the wiring and contact resistances, yielding more accurate results for thin films [27, 28]. The following equation was used to calculate the conductivity:

$$\boldsymbol{\sigma} = \frac{\mathbf{1}}{\mathbf{4.5324}\times\boldsymbol{R_s}\times\boldsymbol{t}}\ \text{S/cm};$$

Where, $\boldsymbol{R_s}$= Sheet resistance (measured by four-point probe), $\boldsymbol{t}$= thickness (measured by profilometer), and 4.5324= correction factor.

2.2.3. Ionic transference number measurement

The GAMRY four-point probe equipment was used to measure the ionic transference number of the samples. In this case, DC polarization method was applied to observe the DC current as a function of time by applying a fixed DC voltage across the sample. The fixed DC voltage was supplied through the tungsten carbide probes of the four-point probe equipment. Table 2 lists the parameters used during the measurement. Similar parameters were applied to all the samples in order to identify the accurate ionic contribution under a constant condition.

Table 2: All the parameters applied to characterize ionic transference number of electrospun PVA: CS membrane immersed in EMIMCl and BMIMBr

DC voltage	Time frame (s)	Maximum current limit (mA)	Temperature (K)
0.1	0-1000	20	303

2.2.4. Seebeck coefficient measurement

The Seebeck coefficient measurement was carried out using an Ozawa Science RZ2000i Instrument. Fig. 2 presents a schematic of the experimental layout. The measurements were taken under a $5x10^{-5}$-Torr vacuum. The sample was wound with Pt wire and mounted horizontally on an electrode for the measurements. Probe leads were connected to the sample by silver paint for improved contact. To generate a temperature gradient, one electrode was heated using a furnace and another was cooled by supplying cold air inside a double-walled quartz tube attached to the electrode. The temperature gradient was established by controlling the flow rate of cold air. The Seebeck coefficients were measured using the Pt wires of the thermocouple through a digital multimeter featuring measurement resistance in the range of 1 Ω to 100 MΩ. The Seebeck coefficients were measured using the ratio between the voltage difference generated and the temperature difference between the hot and cold terminals. For the thermopower measurement, the steady-state direct current method was used. For the conductivity measurement, the two-probe method was applied, in which a DC current passed through the sample using one side of the thermocouples attached to the Pt electrodes and the corresponding voltage between the contact points of Pt wires was measured. By varying the current from -1 to 1 μA, the voltage was measured repeatedly. Using a linear current-voltage curve, the resistance was determined, and the Seebeck coefficient was evaluated from the linear temperature gradient-voltage curve. Data points having a linearity over 90% were taken into account as the most reliable points. The measured resistances of the sample were 62±2 kΩ. Throughout the experiment, the temperatures at the hot and cold terminals were taken using a Pt wire thermocouple.

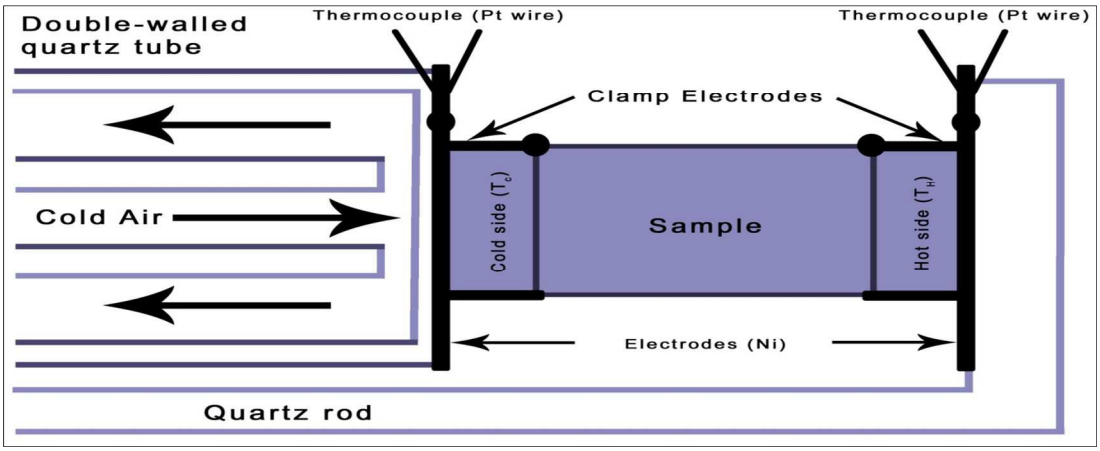

Fig. 2 – Schematic diagram of the Seebeck coefficient measurement experiment (adapted from the layout of the Ozawa Science RZ2000i manual).

2.2.5. Fourier-Transform Infrared (FTIR) Spectroscopy measurement

FTIR spectroscopy was used to analyse the chain interactions between the electrospun films and RTILs through the identification of absorption bands related to the vibrations of functional groups present in PVA, CS, and EMIMCl and BMIMBr macromolecules. A Perkin Elmer Spectrum 400 FTIR spectrometer was used to obtain the FTIR spectra with 1 cm^{-1} resolution in transmission mode from wavenumbers 450 cm^{-1} to 4000 cm^{-1}.

3. Results and discussion

3.1. Morphological properties

Fig. 3 presents the SEM image of electrospun PVA: CS membrane before immersing in RTILs. The microscopic image of electrospun PVA: CS membrane showed that the diameters of the nanofibers are in the range of 250 to 500 nm. The scaffolded matrix of the polymer nanofibers provides high porosity/vacant space compared with gel or casted polymer membranes, which facilitates sufficient trapping of RTILs and more frequent movements of ions. This leads to enhanced mobility of the ions, resulting in significantly increased conductivity. Therefore, the conductivity of the electrospun PVA: CS membrane was observed to be increased from 6×10^{-6} S/cm to 0.10 S/cm after immersing in RTILs (details are reported in Table 3).

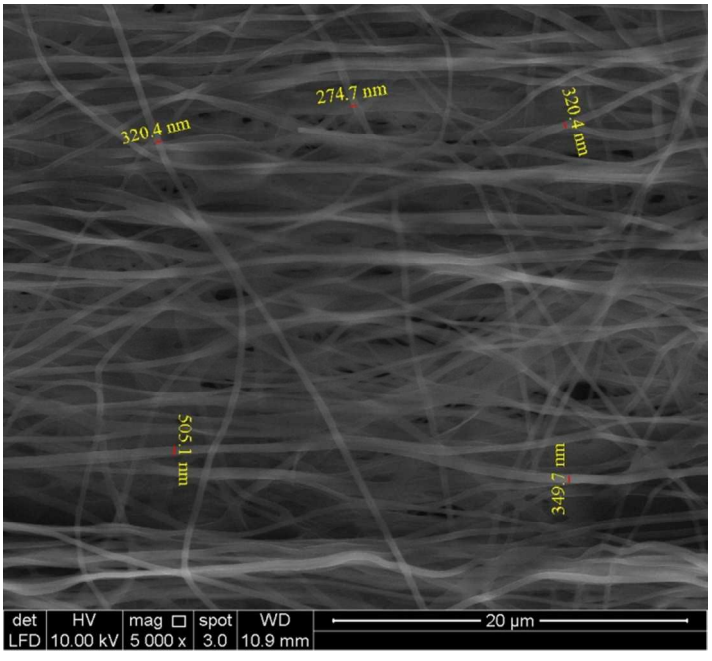

Fig. 3 – SEM image of electrospun PVA: CS nanofibers.

3.2. Conductivity measurements

The conductivity data obtained for electrospun PVA: CS membrane immersed in RTILs are listed in Table 3. The conductivity was observed to increase with increasing molar concentration of RTILs. The maximum conductivity of 0.10 S/cm was achieved for the electrospun PVA: CS membrane immersed in 2 mol/L EMIMCl. The most interesting observation in this study was the maximum electrical conductivities, which surpassed those of the corresponding pure RTILs. For instance, the conductivity of pure RTIL BMIMBr is 5.0×10^{-4} S/cm [29], compared with the value of 4.32×10^{-2} S/cm for PVA:CS membrane immersed in 2 mol/L BMIMBr, representing an increase in the conductivity beyond that of the pure RTIL. A possible explanation of this observation is the "breathing polymeric chain model", in which the inherent folding and unfolding of the polymer chains induce fluctuations at the microscopic level inside the polymer matrix, which generates greater ionic motion than in the pure RTILs. In addition, the breathe in and out of the polymer chains constantly breaks the ion pairs that induces more free charge carriers in the scaffolded matrix of the polymer nanofibers, resulting in significantly increased conductivity [30]. When the concentration of ILs was increased to more than 2 mol/L, there was the challenge of adequately drying the membrane. The hygroscopic nature of the ILs trapped the water molecule at high concentrations, thus causing high viscosity. Therefore, it was resolved that 2 mol/L is the optimum concentration for the membrane.

Table 3: Conductivity data for electrospun PVA:CS membrane immersed in various RTILs with varying concentration

RTIL	Thickness in 1 mol/L (μm)	Thickness in 2 mol/L (μm)	Conductivity in 1 mol/L (S/cm)	Conductivity in 2 mol/L (S/cm)
EMIMCl	**12.91**	**13.90**	**5.50×10^{-2}**	**1.02×10^{-1}**
BMIMBr	**8.28**	**9.14**	**4.20×10^{-2}**	**4.32×10^{-2}**

3.3. Transference number analysis

The transference numbers corresponding to ionic (t_{ion}) and electronic (t_{ele}) transports were calculated for electrospun PVA: CS membrane immersed in 2 mol/L EMIMCl and BMIMBr, respectively, because of their exhibiting higher conductivity compare with the other combinations. The transference numbers were calculated from the polarization current versus time plot. In this case the following equations were used: [31, 32]

$$t_{ion} = \frac{(I_i - I_f)}{I_i};$$

and

$$t_{ele} = 1 - t_{ion} ;$$

Where, I_i= Initial current, I_f= Final current, and t_{ion}= ionic transference number. The transference numbers of ions t_{ion} for all the samples lies between 0.65 and 0.70, which in other words proves that $t_{ion} > t_{ele}$ for the electrospun PVA: CS membrane immersed in RTILs. These results suggest that the charge transport in this system is dominated by ions [32, 33]. Table 4 lists the ionic transference numbers calculated for all the samples. Fig. 4 and Fig. 5 demonstrate the polarization current versus time plots of the electrospun PVA: CS membrane immersed in RTILs EMIMCl and BMIMBr, respectively.

Table 4: Transference number data of electrospun PVA: CS membrane immersed in RTILs EMIMCl and BMIMBr

RTIL	Initial Current (A)	Final Current (A)	Ionic Transference Number
EMIMCl	**6.55×10^{-7}**	**1.92×10^{-7}**	**0.70**
BMIMBr	**1.07×10^{-5}**	**3.75×10^{-6}**	**0.65**

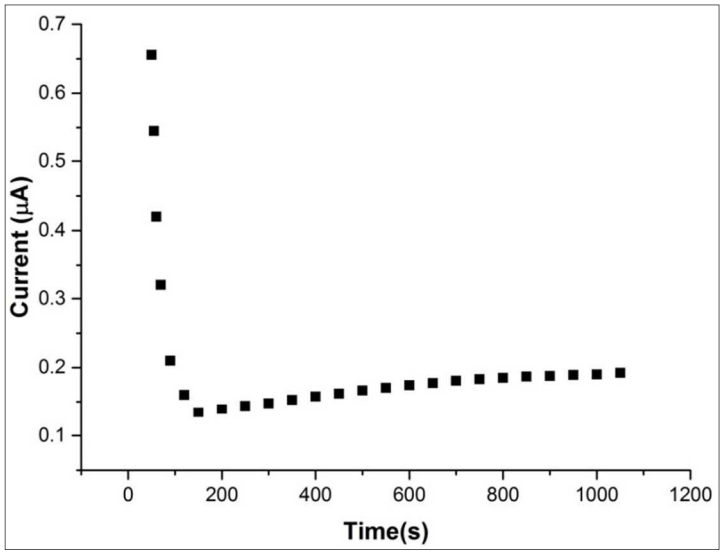

Fig. 4 – DC polarization current versus time plots for PVA: CS membrane immersed in 2 mol/L EMIMCl.

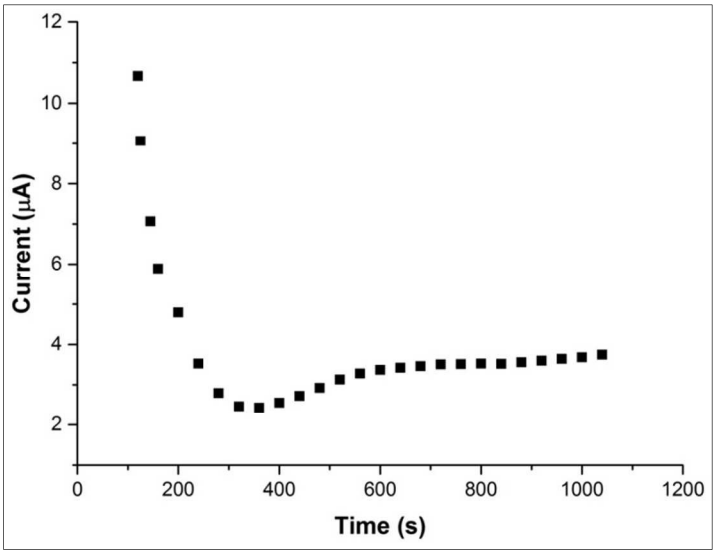

Fig. 5 – DC polarization current versus time plots for PVA: CS membrane immersed in 2 mol/L BMIMBr.

3.4. Thermoelectric potential of the electrospun ionic liquid membrane

Doping is an important means to yield high conductivity, and thus a higher optimized Seebeck coefficient, in polymers. A significant advantage of doping is the conformation of the conducting host molecules, which consequently modify the carrier transport properties in the polymer matrix [34]. For the Seebeck coefficient measurement, the PVA: CS membrane immersed in 2 mol/L EMIMCl was considered because of it exhibiting the maximum conductivity compared with other combinations reported in Table 3. The Seebeck coefficients were measured in the temperature range of 298 K to 318 K as polymer thermoelectric materials are usually targeted for the low temperature applications. The maximum Seebeck coefficient of 17.92 μV/K was obtained at 300.7 K, with an average of 14.9 μV/K. All the Seebeck coefficients were observed to be negative. The negative values of the Seebeck coefficients are thought to be due to the fact the ionic liquid dissociates into cations and anions in the PVA: CS nanofiber scaffolded matrix, where the anions (Cl^-) are expected to have higher mobility than the cations ($C_6H_{11}N_2^+$). This is in turn thought to be due to the lower mass of the (Cl^-) ions, and thus the negatively charged anions act as the majority charge carriers, resulting in the negative Seebeck coefficient [35, 36]. However, for the practical implementation as a thermoelectric generator, a redox couple has to be incorporated with RTILs in order to allow charge transfer from the electrospun membrane to the electrode and vice versa [35, 37]. Fig. 6 presents the Seebeck coefficient as a function of temperature.

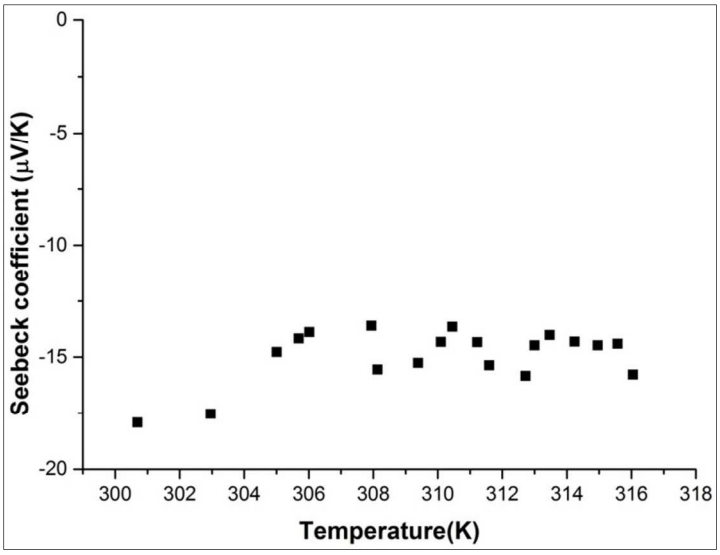

Fig. 6 – Seebeck coefficients for PVA: CS membrane immersed in 2 mol/L EMIMCl.

3.5. FTIR analysis

In this study, extensive FTIR analysis has been carried out with all possible variations. Because both PVA and CS polymers are capable of forming hydrogen bonds, it is expected that some identical interactions could occur between the different molecular groups. The FTIR spectra of pure PVA, CS, and electrospun PVA: CS is shown in Fig. 7a. FTIR spectra of electrospun PVA: CS and electrospun PVA: CS immersed in EMIMCl and BMIMBr are shown in Fig. 7b and 7c, respectively. For pure PVA, the stretching and bending of the hydroxyl (–OH) group are observed at approximately 3300 cm^{-1} and 1377 cm^{-1}, respectively. An asymmetric stretching vibration was noted at approximately 2945 cm^{-1}, which represents the methylene group (CH_2). The band at approximately 1100 cm^{-1} signifies C–O stretching, and the band at approximately 1740 cm^{-1} corresponds to the C=O stretching of acetyl groups that exist on the PVA backbone [38-41]. In the spectra of pure CS, the saccharide structures, which are regarded as the main characteristic bands, were observed at approximately 1035 cm^{-1} and 1150 cm^{-1}. Weaker amino group bands were observed at approximately 1250 cm^{-1}. Strong characteristic amino bands were observed at approximately 3400 cm^{-1}, 1672 cm^{-1}, and 1595 cm^{-1}, which correspond to –OH stretching, amide I, and amide II bands, respectively[18, 21].

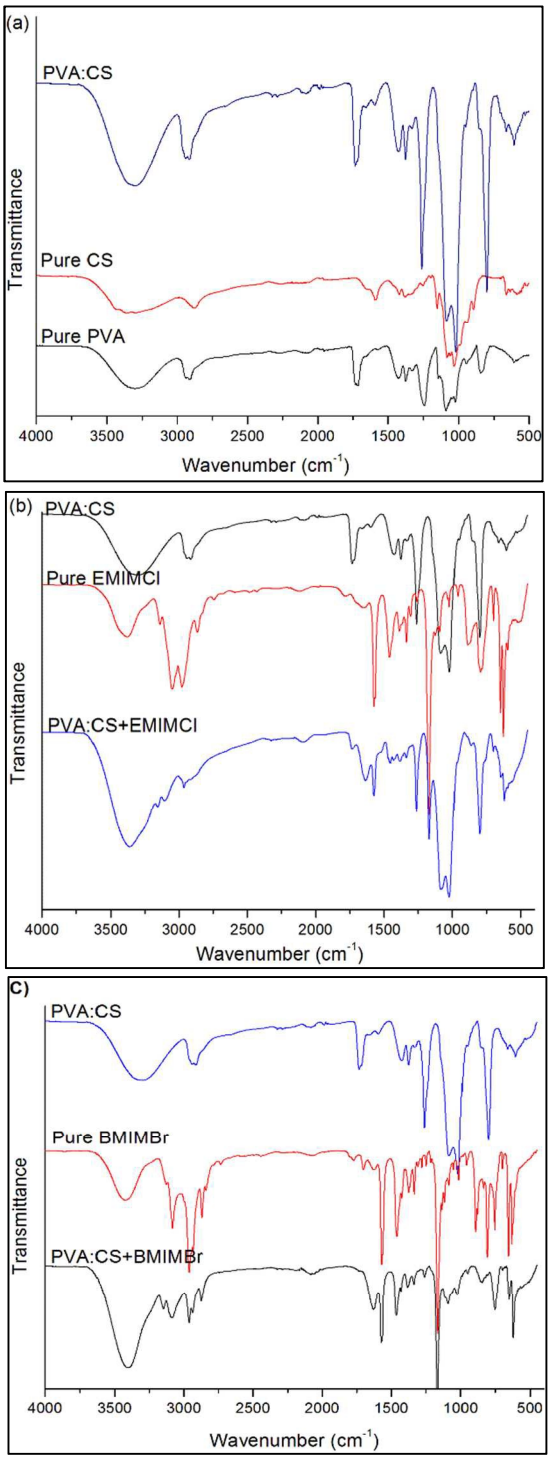

Fig. 7. FTIR spectra of (a) pure PVA, CS, and electrospun PVA: CS; (b) electrospun PVA: CS immersed in EMIMCl, pure EMIMCl, and electrospun PVA: CS; (c) electrospun PVA: CS immersed in BMIMBr, pure BMIMBr, and electrospun PVA: CS.

In the spectra of electrospun PVA: CS membrane, the absorption peak at 1250 cm^{-1} was absent unlike in the FTIR spectra of pure CS. Furthermore, the bands at approximately 1028 cm^{-1} and 1093 cm^{-1} represent a primary amine and –OH group with polymeric association, which indicate the hydrogen bond conformation between the two polymers (PVA and CS) in the electrospun PVA: CS membrane [20, 21]. For pure EMIMCl, the peaks at 3050 cm^{-1} were assigned as the asymmetric –CH3 group attached to the imidazolium ring. Peaks at 2974 were assigned as asymmetric stretching of the aliphatic $–CH_3$ group and 2866 cm^{-1} for the symmetric stretching of the $–CH_2$ group [42]. A broad peak in the range of 3500-3250 cm^{-1} is due to the quaternary amine salt formation with the chlorine ion. Peaks at 1664 and 1330 cm^{-1} are due to C=C and C=N stretching respectively[43]. For pure BMIMBr, the peaks at 3082 cm^{-1} is represented by the asymmetric $–CH_3$ group attached to the imidazolium ring. The aliphatic $–CH_3$ and $–CH_2$ groups resonated at 2961 and 2869 cm^{-1} respectively. A broad peak 3600-3300 cm^{-1} represents the formation of quaternary amine salt with bromide ion. In addition, the $EMIM^+$ cation was observed to be dominated by a strong isolated band at 1164 cm^{-1}, whereas the band at 1170 cm^{-1} represents the $BMIM^+$ cation [44-46]. In the spectra of the electrospun PVA: CS immersed in EMIMCl and BMIMBr, we observed no specific chemical bonding between the polymer scaffolded nanofiber matrix and RTIL. The RTILs are physically disperse in a polymer scaffolded nanofiber matrix, [47] for the case of the PVA:CS nanofiber scaffolded membrane immersed in RTILs.

4. Conclusion

A novel approach to generate electrically conductive electrospun polymer membrane has been presented in this study. Followings are the key findings of this approach:

- The electrospun polymer membrane was found to act as a scaffold for trapping the RTILs, thus successfully enhancing the conductivity up to 0.10 S/cm.
- The maximum electrical conductivities achieved through this method were found to surpass those of the corresponding pure RTILs, which is thought to be due to the folding and unfolding of the polymer chains.
- The ionic transference number results suggest that the charge transport in this system is dominated by ions.
- FTIR results showed that the RTILs are physically dispersed in the polymer nanofiber matrix.
- By achieving a Seebeck coefficient of up to 17.92 μV/K, the presented method shows potential as a polymer-based TE material, implying its feasibility for use in low-temperature/flexible applications.

The advantage of this approach is that it provides a simple fabrication technique that may be used as a starting concept to produce relatively highly electrically conductive polymers, which might also be of use as materials for other energy conversion devices, such as dye-sensitized solar cells and sensors.

Acknowledgements

This research is supported by the University of Malaya–Ministry of Higher Education Grant UM.C/625/1/HIR/MOHE/ENG/29, University of Malaya Research Grant (UMRG) RP014D-13AET, the University of Malaya Science Fund (06/01/03/SF0831), and the University of Malaya FRGS (Grant No. FP035-2013A).

References

1. B. P. Sautter, *Continuous Polymer Nanofibers Using Electrospinning*, University of Illinois, Chicago, 2005.
2. G. S. M. Chowdhury, *International Journal of Basic & Applied Sciences IJBAS-IJENS*, 2010, **10,** No. 06.
3. E. Zussman, A. Theron and A.L. Yarin, *Applied Physics Letter*, 2003, **82**, 973–975
4. H. Li, Y. Bai, F. Wu, Y. Li and C. Wu, *Journal of Power Sources*, 2015, **273**, 784-792.
5. Y. Bai, Z. Wang, C. Wu, R. Xu, F. Wu, Y. Liu, H. Li, Y. Li, J. Lu and K. Amine, *ACS Appllied Materials. Interfaces*, 2015, **7**, 5598−5604.
6. A. Martins, R. L. Reis and N. M. Neves, *International Materials Reviews*, 2008, **53**, 257-274.
7. N. Kattamuri, J.H. Shin, B. Kang, C. G. Lee, J. K. Lee and C. Sung, *Journal of Materials Science*, 2005, 40, 4531–4539.
8. H. F. Jia, G. Y. Zhu, B. Vugrinovich, W. Kataphinan, D. H. Reneker and P. Wang, *Biotechnology Progress*, 2002, **18**, 1027–1032.
9. K. Kim, M. Yu, X. Zong, J. Chiu, D. Fang, B. S. Hsiao, B. Chu and M. Hadjiargyrou, *Biomaterials* 2003, 24, 4977–4985.
10. X. Wang, Y. G. Kim, C. Drew, B. C. Ku, J. Kumar and L. A. Samuelson, *Nano Letter*, 2004, **4**, 331–334.
11. Y. Z. Zhang, J. Venugopal, Z.M. Huang, C. T. Lim and S. Ramakrishna, *Polymer*, 2006, **47**, 2911–2917.
12. S. Ramakrishna, K. Fujihara, W. E. Teo, T. Yong, Z. Ma and R. Ramaseshan, *Materials Today*, 2006, **9**, 40–50.

13. Z.-M. Huang, Y. Z. Zhang, M. Kotaki and S. Ramakrishna, *Composites Science and Technology*, 2003, **63**, 2223-2253.

14. J. Xie, X. Li and Y. Xia, *Macromolecular Rapid Communications*, 2008, **29**, 1775-1792.

15. I. S. Chronakis, S. Grapenson and A. Jakob, *Polymer*, 2006, **47**, 1597-1603.

16. W. Zhou and H. Yu, *ACS Applied Materials & Interfaces*, 2012, **4**, 2154-2159.

17. L. Meli, J. Miao, J. S. Dordick and R. J. Linhardt, *Green Chemistry*, 2010, **12**, 1883-1892.

18. A. Islam, T. Yasin and I. U. Rehman, *Radiation Physics and Chemistry*, 2014, **96**, 115-119.

19. M. Pakravan, M.-C. Heuzey and A. Ajji, *Polymer*, 2011, **52**, 4813-4824.

20. M. H. Buraidah and A. K. Arof, *Journal of Non-Crystalline Solids*, 2011, **357**, 3261-3266.

21. J. Bonilla, E. Fortunati, L. Atarés, A. Chiralt and J. M. Kenny, *Food Hydrocolloids*, 2014, **35**, 463-470.

22. N. J. English, D. A. Mooney and S. O'Brien, *Molecular Physics*, 2011, **109**, 625-638.

23. T. Tsuda and C. L. Hussey, *Interface*, 2007, **16**, 42-49.

24. U. Domańska, *Pure and Applied Chemistry*, 2005, **77**, 543-557.

25. M. T. Viciosa, H. P. Diogo and J. J. M. Ramos, *RSC Advances*, 2013, **3**, 5663-5672.

26. H. Homayoni, S. A. H. Ravandi and M. Valizadeh, *Carbohydrate Polymers*, 2009, **77**, 656-661.

27. S. Ling, W. Jianjun and B. Elmar, *Scientific Reports*, 2013, **3**.

28. C.H. Chen, J. C. LaRue, R. D. Nelson, L. Kulinsky and M. J. Madou, *Journal of Applied Polymer Science*, 2012, **125**, 3134-3141.

29. P. N. N. Tshibangu, Silindile Nomathemba; Dikio, Ezekiel Dixon, *International Journal of Electrochemical Science*, 2011, **6**. 2201-2213.

30. S. Chandra, S. S. Sekhon and N. Arora, *Ionics*, 2000, **6**, 112-118.

31. M. Hema, S. Selvasekerapandian, A. Sakunthala, D. Arunkumar and H. Nithya, *Physica B: Condensed Matter*, 2008, **403**, 2740-2747.

32. Z. Osman, M. I. Mohd Ghazali, L. Othman and K. B. Md Isa, *Results in Physics*, 2012, **2**, 1-4.

33. D. Kumar and S. A. Hashmi, *Solid State Ionics*, 2010, **181**, 416-423.

34. G. H. Kim, L. Shao, K. Zhang and K. P. Pipe, *Nature Materials*, 2013, **12**, 719-723.

35. S. Uhl, E. Laux, T. Journot, L. Jeandupeux, J. Charmet and H. Keppner, *Journal of Elec Materi*, 2014, **43**, 3758-3764.

36. R. S. Datta, S. M. Said, S. R. Sahamir, M. R. Karim, M. F. M. Sabri, T. Nakajo, M. Kubouchi, K. Hayashi and Y. Miyazaki, *Journal of Elec Materi*, 2014, **43**, 1585-1589.

37. T. J. Abraham, D. R. MacFarlane and J. M. Pringle, *Chemical Communications*, 2011, **47**, 6260-6262.

38. M. N. Hyder and P. Chen, *Journal of Membrane Science*, 2009, **340**, 171-180.

39. E. M. Abdelrazek, I. S. Elashmawi and S. Labeeb, *Physica B: Condensed Matter*, 2010, **405**, 2021-2027.

40. E. Souza Costa-Júnior, M. Pereira and H. Mansur, *J Mater Sci: Mater Med*, 2009, **20**, 553-561.

41. H. S. Mansur, R. L. Orefice and A. A. P. Mansur, *Polymer*, 2004, **45**, 7193-7202.

42. J. Yoonnam, S. Jaeho, K. Doseok, S. Chungwon, C. Hyeonsik, O. Yukio, O. Ryosuke and H. Hiro-o, *J. Phys. Chem. B,* 2008, **112**, 923-928.

43. S. A. Dharaskar, M. N. Varma, D. Z. Shende, C. K. Yoo, and K. L. Wasewar, *Scientific World J.*, 2013, **2013**, 1-9.

44. T. Rajkumar and G. Ranga Rao, *J Chem Sci*, 2008, **120**, 587-594.

45. C. J. Johnson, J. A. Fournier, C. T. Wolke and M. A. Johnson, *The Journal of Chemical Physics*, 2013, **139**, 224305 (1-7).

46. D. H. Williams and I. Fleming, *SPECTROSCOPIC METHODS IN ORGANIC CHEMISTRY*, 6th edn., 2007.

47. S. Uk Hong, D. Park, Y. Ko and I. Baek, *Chemical Communications*, 2009, 7227-7229.

Graphical Abstract